RSC Advances

ROYAL SOCIETY OF CHEMISTRY

www.rsc.org/advances

Non-enzymatic glucose electrochemical sensor based on silver nanoparticles decorated organic functionalized multiwall carbon nanotubes

Ali A. Ensafi*, N. Zandi-Atashbar, B. Rezaei, M. Ghiaci, M. Esmaeili Chermahini, P. Moshiri

Department of Analytical Chemistry, College of Chemistry, Isfahan University of Technology, Isfahan 84156–83111, Iran

Abstract

An efficient, fast and stable non–enzymatic glucose sensor was prepared by decorating silver nanoparticles on the organic functionalized multiwall carbon nanotubes (AgNPs/F–MWCNTs). MWCNTs were functionalized by organic amine chains and characterized using energy–dispersive X–ray and FT–IR spectroscopy. Moreover, the decorated AgNPs monitored by transmission electron microscopy showed the spherical shapes with the mean size of 9.0±2.8 nm. To further study, the glassy carbon electrode (GCE) was modified by the synthesized compound and the modification evaluation was conducted using cyclic voltammetry and electrochemical impedance spectroscopy. The electrochemical data reveal the modification of GCE leds to easier electron transfer rather than the bare unmodified GCE due to the presence of functionalized MWCNTs in accompany with the electrocatalytic effect of the decorated silver nanoparticles. Furthermore, the suggested modified electrode was applied as a non–enzymatic glucose sensor using electrochemical techniques including cyclic voltammetry and hydrodynamic chronoamperometry. The results obtained from the amperometric

*Corresponding author: Fax: +98–31–33912350; Tel.: +98–31–33913269; E–mail: Ensafi@cc.iut.ac.ir; Ensafi@yahoo.com; aaensafi@gmail.com

analysis of glucose in 0.1 M NaOH solution indicated the efficient performance of the electrode with a low detection limit of 0.03 μM and high sensitivity of 1057.3 μA mM^{-1}, as well as a linear dynamic range of 1.3 to 1000 μM. The practical application of this sensor was also examined by analyzing glucose in the presence of common interfering species existing in a real sample of human blood serum.

Keywords: Non–enzymatic glucose sensor; Silver nanoparticles–organic functionalized multiwall carbon nanotubes; Amperometry.

1. Introduction

Diabetes and its serious health complications have found the main position in medicinal sciences, as a principal humanity challenge. Thus, each influential factor, such as the levels of insulin and glucose in human blood should be investigated.[1] Insulin has been determined using various analytical methods, especially electrochemistry.[2] Moreover, since the level of glucose in blood should be critically regulated, usually in the range of 3.0–8.0 mM,[3] different approaches have been purposed to measure it, including spectroscopy,[4] spectrofluorimetry,[5] electrochemistry,[3] and chromatography.[6] Within these methods, electrochemical sensors have been developed based on enzymatic and non–enzymatic applications.[7] Although enzyme–based sensors represented some advantages such as high selectivity and low detection limit, some drawbacks including poor reproducibility, low thermal and chemical stability and high cost have been reported for these sensors.[8-10] Hence, the studies on enzyme–free electrochemical sensors have been developed as a result of electrode modification. Metal nanomaterials because of their high surface areas and electrocatalytic properties have been used as the modifier for glucose detection.[11-14] Moreover, these properties can be improved by stabilizing the

nanoparticles on the proper support. Multiwall carbon nanotubes (MWCNTs), due to excellent conductivity, good chemical stability, large surface-volume ratio, and high adsorption capacity, have been utilized as the nanoparticles support.[15,16] However, the nanoparticles decorated on the bare MWCNTs can be removed from it, because of absence of strong interactions between them, in repeatable usages, whereas the covalent functionalization of MWCNTs with organic ligands can more effectively load the nanoparticles.[16-18]

Herein, silver nanoparticles (AgNPs) decorated on new synthesized functionalized MWCNTs were employed as a new non–enzymatic sensor to detect glucose. This modifier was synthesized based on step by step organic bonding to functionalized MWCNTs. The synthesis was characterized using Fourier transform infrared (FT–IR) spectroscopy, transmission electron microscopy (TEM), cyclic voltammetry (CV) and electrochemical impedance spectroscopy (EIS). Moreover, the sensing performance of the synthesized modifier was studied by hydrodynamic chronoamperometry. The resulted data showed high sensitive and selective in accompany with a fast analysis of glucose. At last, in this work, the reliability of the sensor for real sample analysis was examined using human blood serum samples.

2. Experimental

2.1. Reagents

Sliver nitrate ($AgNO_3$), glucose, sodium hydroxide (NaOH), phosphoric acid (H_3PO_4) and sucrose were purchased from Merck. Ascorbic acid, uric acid, fructose and multiwall carbon nanotubes (MWCNTs) were supplied from Sigma–Aldrich. Phosphate buffer solution (PBS, 0.1 M) at various pHs was prepared by addition of 0.10 M NaOH to 0.10 M H_3PO_4 solution. All the other chemicals were of analytical reagent grade and

used without further purification. All water used for preparing the solutions in this work was double distilled water. Three human blood plasma samples were provided from Alzahra Hospital (Isfahan, Iran). The proteins contained in the plasma were filtered as pretreatment of real samples.

2.2. Apparatus

The products obtained from each step of the synthesis, as KBr–mixed pellets, were monitored by recording FT–IR spectra using FT–IR Spectrometer (Jasco, FT/IR–680 Plus). The morphology and size of the generated AgNPs decorated on functionalized MWCNTs were analyzed using a transmission electron microscope (TEM, TECNAI, Model F30, USA). Energy dispersive X–ray spectra (EDX) were recorded with a Philips XLC instrument.

All electrochemical experiments were done using a common three-electrode system (Autolab, PGSTAT–30 potentiostat/galvanostat, Eco–Chemie, Netherlands). The modified glassy carbon electrode (GCE), Pt rod and Ag/AgCl/3.0 M KCl were used as working, auxiliary and reference electrodes, respectively. The recorded data were processed applying General Purpose Electrochemical System (GPES, version 4.9) and Frequency Response Analyzer (FRA). All electrochemical experiments were studied after stabilizing the surface of the electrode by operation of 20 cycles in the potential window of –1.00 to +1.00 (V *vs.* Ag/AgCl). Cyclic voltammograms were recorded at various pH solutions of PBS and 0.1 M NaOH with a scan rate of 100 mV s^{-1}, which the results were optimized in the alkaline medium of NaOH. Thus, the amperometric measurements were conducted at a hydrodynamic electrode by sequential addition of glucose solution to 0.1 M NaOH solution. The electron transfer resistances of the electrodes were measured by electrochemical impedance spectroscopy (EIS). All EIS

studies were done with a frequency range of 0.01 Hz to 100 kHz, the amplitude wave potential of 10 mVand 0.20 Vas an applying potential in a 10.0 mM $Fe(CN)_6^{3-/4-}$solution, as a probe. All these electrochemical measurements were carried out at ambient temperature.

2.3. Procedure

The synthesis of functionalized multiwall carbon nanotubes (F–MWCNTs) is schematically summarized in Fig. 1. MWCNTs were functionalized by refluxing in a mixture of HNO_3 (6.0 M) and H_2SO_4 (2.0 M) for 12 h. Afterwards, the functionalized MWCNTs (CNT–COOH) was continually sufficiently rinsed with distilled water, and then it was dried under vacuum conditions for 12 h. 500 mg of the MWCNTs–COOH was thoroughly dispersed in THF in an ultrasonic bath. After that, 12.0 mL of $SOCl_2$ was added to the former suspension and stirred at room temperature for 24 h. The product of MWCNT–COCl was refluxed with 15.0 mL of ethylenediamine at 60 ^oC for 12 h. The mixture was reacted with 1.0 g cyanuric chloride and 5.0 mL diethylenetriamine in THF under a nitrogen atmosphere to form MWCNT–CO–NH–cyanuric and MWCNT–CO–NH–cyanuric–NH_2, respectively. At last, the F–MWCNTs were prepared by centrifuging and drying MWCNT–CO–NH–cyanuric–NH_2.

0.10 g F–MWCNTs was dispersed in 200 mL distilled water under ultrasonic waves for 30 min. To form Ag(I)/F–MWCNTs, 10.0 mL of $AgNO_3$ solution (1.0 mM) was drop by drop added to F–MWCNTs suspension during 24 h. The AgNPs/F–MWCNTs were prepared by reducing the silver ions to silver nanoparticles (AgNPs) using $NaBH_4$.

3. Results and discussion

3.1 Characterization of synthesized compound

Synthesis of AgNPs/F–MWCNT was characterized using several techniques including energy–dispersive X–ray spectroscopy (EDX), Fourier transform infrared spectroscopy (FT–IR), and transmission electron microscopy (TEM). EDX analysis indicated F–MWCNTs were prepared by the weight percentages of 79.74, 9.68, and 10.58 corresponded to carbon, oxygen, and nitrogen. It confirmed that MWCNTs were satisfactorily functionalized by the organic compound. FT–IR spectra exhibit the steps of organic compound synthesis as can be seen in Fig. 2A. The spectrum (a) of MWCNTs shows the C–C stretching bonds in the range of 1580–1650 cm^{-1} and the peak locating at around 850 $cm^{-1}$is due to the nanotubes symmetrical modes.[19] The bond at 1640 cm^{-1} can be associated with –C=O stretching of the carboxyl group. As shown in the spectra (b and c), this characteristic bond was moved to 1690 and 1630 cm^{-1} by conversion of COOH to COCl and amide group, respectively. As shown in Fig. 2B, the silver nanoparticles (AgNPs) fabricated on F–MWCNTs represented the size distribution of 3.0 to 17.0 nm with the mean size of around 9.0±2.8 nm.

3.2 Electrochemical characterization

The AgNPs/F–MWCNTs were further characterized using cyclic voltammetry (CV) and electrochemical impedance spectroscopy (EIS). In a comparison of the unmodified glassy carbon electrode (GCE), F–MWCNTs–GCE, and AgNPs/F–MWCNTs–GCE, the modification showed the facility of electron transferring as indicated in Fig. 3 (A and B). Accordingly, the cyclic voltammograms recorded in 0.1 M NaOH with a scan rate of 50 mVs^{-1}, as exhibited in Fig. 3A indicates the corresponding the electrochemical oxidation that generates surfaces Ag-oxide layer onto the nanoparticles, i.e. Ag to $Ag^{(I)}$ and $Ag^{(I)}$to $Ag^{(II)}$ [20]. To further confirm the effect of the

modifier, further investigation was conducted using the EIS analysis in 10.0 mM $Fe(CN)_6^{3-/4-}$solution, as a probe. In the Nyquist plots (Fig. 3B), facility of electrical conductivity between the redox probe and the electrode modified was confirmed that the electron is transferring was increasingly improved by the modification of the GCE using F–MWCNTs and AgNPs/F–MWCNTs as the semicircular corresponds to the electron transfer–limited process was decreased. On the other words, the charge transfers resistance (R_{ct}) at the surface of the electrode was decreased because of the good conductivity of AgNPs/F–MWCNTs, which it could make electron transfer easier.

3.3. Electroanalysis of glucose at AgNPs/F–MWCNTs–GCE

Analysis of glucose was studied using AgNPs/MWCNTs–GCE compared to non AgNPs decorated F–MWCNTs and bare GCEs, as showed in Fig. 4. The electrocatalytic effect of AgNPs/MWCNTs resulted in a significant increase the oxidation currents in the presence of glucose compared to the results obtained from two other unmodified electrodes. Thus, the further investigations for glucose sensing were performed at AgNPs/MWCNTs–GCE. Fig. 5 shows that the CVs in the presence of 5.0 mM glucose at different scan rates (10 to 300 mV s^{-1}) had a linear relationship between the oxidation currents (in the range of 0.60 to 0.65 V, depends on the scan rate) and the square root of the scan rates (i.e. $v^{1/2}$). This proportional linearity, with a correlation coefficient of 0.995, represented that the mass transfer of glucose at the surface of the electrode was controlled by diffusion, which is perfect for quantitative sensing objectives.

3.4. Chronoamperometric study of AgNPs/F–MWCNTs–GCE in the presence of glucose

Chronoamperometric responses of AgNPs/F–MWCNTs–GCE with a working potential at 0.58 V in 0.1 M NaOH solution for sequential addition of glucose are

displayed in Fig. 6. The further amperometric investigations were performed at 0.58 V due to the lower potential values represented lower increases in amperometric responses and the signal obtained at higher potentials could be affected by interfering species, as well as were less stable against glucose concentration, so, 0.58 V was selected as the optimum potential. Moreover, the signal obtained from glucose injection quickly become stable with a response time of less than 3s. According to Fig. 6, two linear ranges of calibration were observed: at the lower glucose concentration range from 1.3 to 1000 μM, with regression of I(μA) = 31.720C(mM) – 0.245 and R^2 = 0.998; and at higher glucose concentration range from 1.11 to 4.14 mM, with regression of I(μA) = 3.144C(mM) + 30.370 and R^2 = 0.955. Two linearities may result from the adsorption of intermediate.[21] On the other words, in low glucose concentration, amperometric responses resulted from the oxidation of diffusive glucose, and in higher amounts of glucose the slope of calibration curve was decreased due to adsorption of the oxidation product of glucose, which decreased the active site of AgNPs/F–MWCNTs and hindered the glucose diffusing into the electrode surface.

The limit of detection (LOD) was calculated using signal to noise ratio of three. The sensitivity of the modified electrode related to glucose concentration was measured by the proportion of the calibration slope to the standard deviation of the current steps.[22] Accordingly, using AgNPs/F–MWCNTs–GCE, the LOD, and sensitivity for glucose determination were achieved as 0.03 μM and 1057.3 μA mM, respectively. The analytical figures of merit of this sensor were comparable and even better than those obtained by other reported non–enzymatic sensors, as tabulated in Table 1.

3.5. Repeatability, stability and selectivity of the glucose sensor

To evaluate the performance of AgNPs/F–MWCNTs–GCE for glucose sensing, ten continuous additions of 0.2 mM glucose solution represented the relative standard deviation (RSD%) of 2.2% as can be seen in Fig. 7A. The addition of 0.70 mM glucose concentration in 0.1 M NaOH solution at the surface of modified electrode indicates relatively stable signal until 1000 s with only 6.3% decrease in the amperometric signal in accordance with Fig. 7B. The selectivity of the glucose sensor was examined in the presence of different interference species including sucrose (Su), fructose (Fr), uric acid (UA), ascorbic acid (AA)and dopamine (DA). The physiological level of glucose in human blood plasma is within 3 to 8 mM while the other interference species involving UA, AA, and DA are existent at the content of 0.1 mM, i.e. one 30th of glucose concentration.[3] Moreover, the existence of other carbohydrates, such as sucrose and fructose can affect the performance of AgNPs/F–MWCNTs–GCE rather than glucose. According to Fig. 7C, the influence of presence of interfering compounds including ascorbic acid (AA) (0.07 mM), dopamine (DA) (0.07 mM), uric acid (UA) (0.07 mM), sucrose (Su) (0.70 mM) and fructose (Fr) (0.70 mM) on the amperometric response of 0.70 mM glucose solution at AgNPs/F–MWCNTs–GCE was investigated. The interference study showed that the amperometric signals were insignificantly affected by the two carbohydrates of sucrose and fructose while easy oxidation of three other compounds in alkaline media represented relatively interfering effects on the signals. As mentioned, since the levels of three interfering species of ascorbic acid, uric acid and dopamine are normally too lower than glucose concentration, the low interfering effects of them can be solved by diluting the sample to real ratios of the species in the human blood plasma, i.e. one thirtieth.[3]

3.6. Real sample analysis

To verify the practical application of AgNPs/F–MWCNTs–GCE as a non–enzymatic glucose sensor, a series of protein–filtered human blood serum was examined. The detection of glucose was conducted using standard addition method. In this case, the serum samples were diluted with 0.1 M NaOH solution until the glucose contents were in the range of 61.0–103.0 μM, in the linear range of calibration. The resulting data of amperometric analyses of real samples are summarized in Table 2. These results were satisfactorily comparable with the ones obtained by hospital glucose analyzer.

4. Conclusion

In summary, the applicable of non–enzymatic glucose sensor based on the decoration of silver nanoparticles on the organic functionalized multiwall carbon nanotubes (AgNPs/F–MWCNTs) was investigated. The sensor was characterized using energy–dispersive X–ray spectroscopy, FT–IR spectroscopy, microscopic image of TEM and electrochemical records of cyclic voltammetry, electrochemical impedance spectroscopy, and chronoamperometry. According to the impedance spectra, the performance of GCE was successfully improved by modifying the electrode with AgNPs/F–MWCNTs as decreasing the electron transfer resistance is related to shortening the semicircular diameter. The electrode was employed as a non–enzymatic sensor to measure the glucose level in biological samples, using hydrodynamic chronoamperometry. As interference study, five usual interfering compounds including ascorbic acid, uric acid, dopamine, sucrose, and fructose were examined in the presence of glucose, which these species in the biological levels rather than glucose represented no significant interfering effects on the amperometric response of glucose oxidation. At last, the reliability of the sensor was verified by analyzing glucose level in blood serum samples.

Acknowledgements

The authors wish to thank Isfahan University of Technology (IUT) Research Council and Center of Excellence in Sensor and Green Chemistry for their support. The authors would like to thanks to Al–Zahra Hospital (Isfahan, Iran) due to the preparation of the real samples.

References

1 C.D.A. Stehouwer, I. Ferreira, M. Kozakova andC. Palombo, Glucose Metabolism, Diabetes, and the Arterial Wall, in: P.M. Nilsson, M.H. Olsen and S. Laurent (Eds), Early Vascular Aging (EVA): New Directions in Cardiovascular Protection, Academic Press, Boston, 1st Edition, 2015, p.p. 147–156.

2 A. Arvinte, A.C. Westermann, A.M. Sesay and V. Virtanen, *Sens. Actuator B Chem.*, 2010, **150**, 756.

3 A.A. Ensafi, M. Mokhtari Abarghoui and B. Rezaei, *Electrochim. Acta*, 2014, **123**, 219.

4 M. Goodarzi and W. Saeys, *Talanta*, 2016, **146**, 155.

5 M. Aloraefy, T.J. Pfefer, J.C. Ramella–Roman and K.E. Sapsford, *Sensor*, 2014, **14**, 12127.

6 M. Grembecka, A. Lebiedzińska and P. Szefer, *Microchem. J.*, 2014, **117**, 77.

7 S.A. Zaidi and J.H. Shin, *Talanta*, 2016, **149**, 30.

8 J. Lin, C. He, Y. Zhao and S. Zhang, *Sens. Actuator B Chem.*, 2009, **137**, 768.

9 X. Kang, Z. Mai, X. Zou, P. Cai and J. Mo, *Anal. Biochem.*, 2007, **363**, 143.

10 X. Li, Q. Zhu, S. Tong, W. Wang and W. Song, *Sens. Actuator B Chem.*, 2009, **136**, 444.

11 J. Chen, Q. Sheng and J. Zheng, *RSC Adv.*, 2015, **5**, 105372.

12 J. Yang, X. Liang, L. Cui, H. Liu, J. Xie and W. Liu, *Biosens. Bioelectron.*, 2016, **80**, 171.

13 Y. Liu, X. Zhang, D. He, F. Maa, Q. Fua and Y. Hu, *RSC Adv.*, 2016, **6**, 18654.

14 X. Luo, Z. Zhang, Q. Wan, K. Wu and N. Yang, *Electrochem. Commun.*, 2015, **61**, 89.

15 U. Yaqoob, A.S.M.I. Uddin and G.–S. Chung, *Sens. Actuator B Chem.*, 2016, **224**, 738.

16 Y. Wang, S. Zhang, W. Bai and J. Zheng, *Talanta*, 2016, **149**, 211.

17 H. Sadegh and R. Shahryari-ghoshekandi, *Nanomed. J.*, 2015, **2**, 231.

18 R. Devasenathipathy, C. Karuppiah, S.-M. Chen, S. Palanisamy, B.-S. Lou, M.A. Ali and F.M.A. Al-Hemaid, *RSC Adv.*, 2015, **5**, 26762.

19 T. Belin and F. Epron, *Mater. Sci. Eng. B*, 2005, **119**, 105.

20 N. Zandi–Atashbar, B. Hemmateenejad and M. Akhond, *Analyst*, 2011, **136**, 1760.

21 L. Qian, J. Mao, X. Tian, H. Yuan and D. Xiao, *Sens. Actuator B Chem.*, 2013, **176**, 952.

22 A.A. Ensafi, N. Zandi-Atashbar, M. Ghiaci, M. Taghizadeh and B. Rezaei, *Mater. Sci. Eng. C*, 2015, **47**, 290.

23 X.-W. Liu, P. Pan, Z.-M. Zhang, F. Guo, Z.-C. Yang, J. Wei and Z. Wei, *J. Electroanal. Chem.*, 2016, **763**, 37.

24 Y. Zhang, E. Zhou, Y. Li and X. He, *Anal. Methods*, 2015, **7**, 2360.

25 R.M.A. Tehrani and S.A. Ghani, *Biosens. Bioelectron.*, 2012, **38**, 278.

26 H.F. Cui, J.S. Ye, W.D. Zhang, C.M. Li, J.H.T Luong and F.S. Sheu, *Anal. Chim. Acta*, 2007, **594**, 175.

27 J. Huang, Z. Dong, Y. Li, J. Li, J. Wang, H. Yang, S. Li, S. Guo, J. Jin and R. Li, *Sens. Actuator B Chem.*, 2013, **182**, 618.

28 Z.-X. Cai, C.-C. Liu, G.-H. Wu, X.-M. Chen and X.I. Chen, *Electrochim. Acta*, 2013, **112**756.

29 R. Sedghi and Z. Pezeshkian, *Sens. Actuator B Chem.*, 2015, **219**, 119.

30 S. Masoomi-Godarzi, A.A. Khodadadi, M. Vesali-Naseh and Y. Mortazavi, *J. Electrochem. Soc.*, 2014, **161**, B19.

Table 1. Performance of the various reported functionalized MWCNTs nonenzymatic modified electrodes for glucose detection.

Sensor	Response time (s)	Applied potential (V)	Linear range (μM)	Detection limit (μM)	Literature
CuO/MWCNTs	3	0.55	4–5000	4.0	23
$CuFe_2O_4$/MWCNTs	5	0.40	0.5–1400	0.2	24
RuO_2/MWCNTs–	–	0.50	500–50000	33	25
Pt–PbNPs/MWCNTs	12	0.30	Up to 11000	1.8	26
Cu/MnO_2/MWCNTs	3	0.60	10–1000	0.17	16
CuNWs[a]/MWCNTs	1	0.55	Up to 3000	0.26	27
PdNPs/MWCNTs	3	0.025	1000–10000	–	28
MWCNTs-COOH-P2AT[b]-Au NPs	–	–	100–3000	3.7	29
Fe_3O_4/MWCNTs	12	0.50	500–7000	15.0	30
AgNPs/F–MWCNTs	3	0.58	1.3–1000 and 1100–4140	0.03	This work

a: Cu nanowires; b: Poly(2-aminothiophenol)

Table 2. Determination of glucose level in real samples using the AgNPs/F–MWCNTs–GCE non–enzymatic sensor.

Sample	Referenced values[a](μM)	Determined values (μM)	RSD (%)
Human serum 1	61.4	62.9	2.4
Human serum 2	112.2	110.6	3.8
Human serum 3	85.7	87.3	3.1

[a] The values provided by the hospital with a relative population standard deviation of 5%.

Legends for the figures:

Fig. 1. The schematic synthesis steps of organic chain functionalized multiwall carbon nanotubes (F–MWCNTs).

Fig. 2. (A):FT–IR spectra of products formed in each step of F–MWCNTs synthesis (CNT–COOH (a), CNT–COCl (b), and CNT–CO–NH–cyanuric–NH_2 (c)); (B): TEM image of AgNPs/F–MWCNTs and size distribution of generated nanoparticles.

Fig. 3. (A): Cyclic voltammograms of GCE (a), F–MWCNTs–GCE (b), and AgNPs/F–MWCNTs (c) in 0.1 M NaOH with scan rate of 50 mVs^{-1}; (B): Nyquist plots of GCE (a), F–MWCNTs–GCE (b), and AgNPs/F–MWCNTs (c) in 10.0 mM $Fe(CN)_6^{3-/4-}$solution with a frequency range of 0.01 Hz to 100 kHz and the amplitude wave potential of 10 mV.

Fig. 4. Cyclic voltammograms of GCE (A), F–MWCNTs–GCE (B), and AgNPs/F–MWCNTs–GCE (C) in 0.1 M NaOH solution in the absence of glucose (a) and in the presence of 2.5 mM glucose solution at a scan rate of 50 mV s^{-1} (b).

Fig. 5. The study of AgNPs/F–MWCNTs–GCE in 0.1 M NaOH solution and the presence of 5.0 mM glucose at the potential scan rate of 10–300 mV s^{-1}. Inset: plot of the oxidation peaks *vs.* the square root of scan rates.

Fig. 6. Current–time study of AgNPs/F–MWCNTs–GCE *vs.* glucose addition in 0.1 M NaOH solution using hydrodynamic electrode at applied potential of 0.58 V vs. Ag/AgCl and 1200 rpm with the corresponding two linear ranges of the calibration curve, showing in the inset.

Fig. 7. Chronoamperometric study of the glucose oxidation current at AgNPs/F–MWCNTs–GCE in 0.1 M NaOH solution based on 10 successive additions of glucose solution (0.20 mM) (A); stability of the signal sensor until 1000 s by addition of glucose solution (0.70 mM) (B); and selectivity of the glucose sensor towards glucose solution (0.70 mM) in the presence of interfering species including sucrose (Su) (0.70 mM), fructose (Fr) (0.70 mM), Uric acid (UA) (0.07 mM), ascorbic acid (AA) (0.07 mM), and dopamine (DA) (0.07 mM) (C).

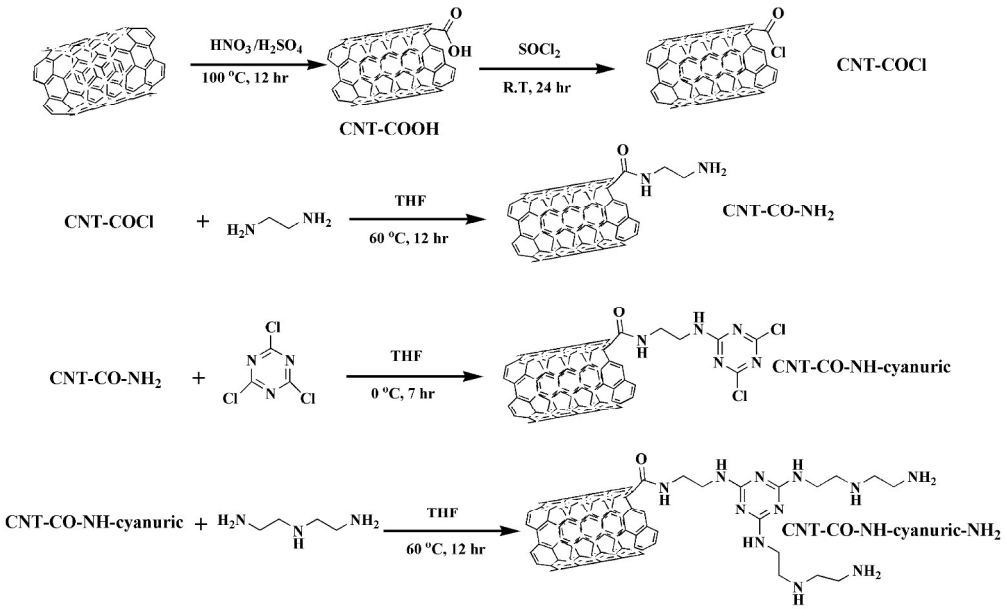

Fig. 1. The schematic synthesis steps of organic chain functionalized multiwall carbon nanotubes (F–MWCNTs).
401x244mm (300 x 300 DPI)

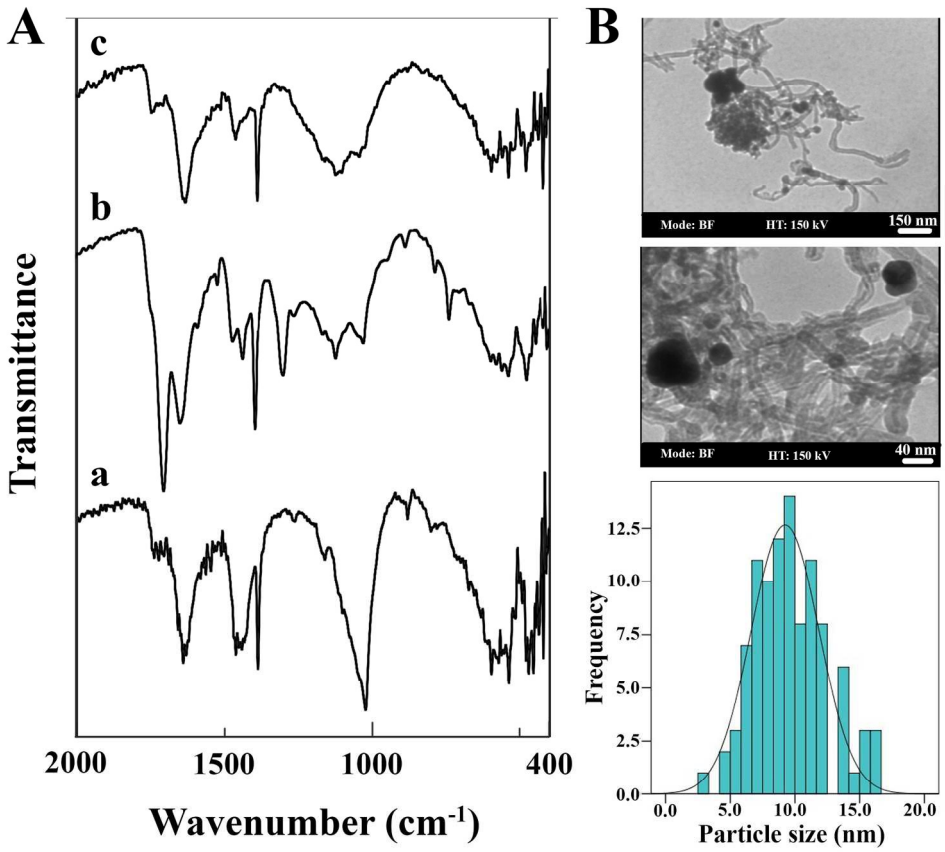

Fig. 2. (A):FT–IR spectra of products formed in each step of F–MWCNTs synthesis (CNT–COOH (a), CNT–COCl (b), and CNT–CO–NH–cyanuric–NH2 (c)); (B): TEM image of AgNPs/F–MWCNTs and size distribution of generated nanoparticles.
199x177mm (300 x 300 DPI)

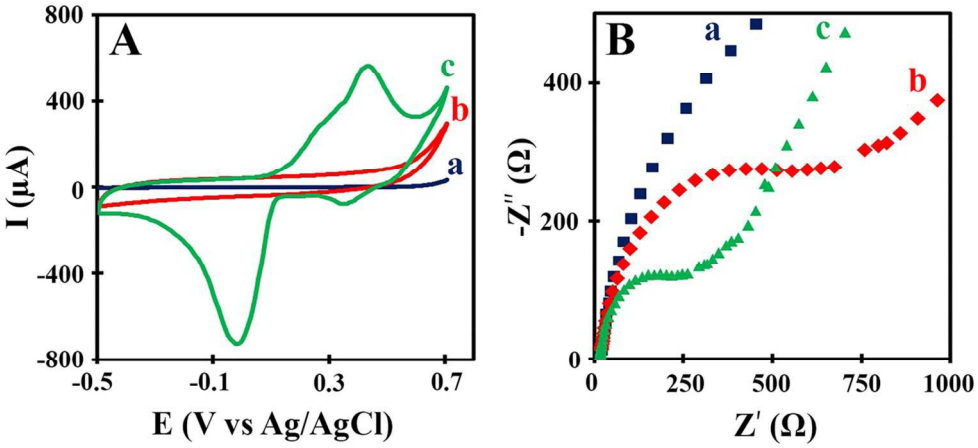

Fig. 3. (A): Cyclic voltammograms of GCE (a), F–MWCNTs–GCE (b), and AgNPs/F–MWCNTs (c) in 0.1 M NaOH with scan rate of 50 mVs–1; (B): Nyquist plots of GCE (a), F–MWCNTs–GCE (b), and AgNPs/F–MWCNTs (c) in 10.0 mM Fe(CN)63–/4–solution with a frequency range of 0.01 Hz to 100 kHz and the amplitude wave potential of 10 mV.
119x57mm (300 x 300 DPI)

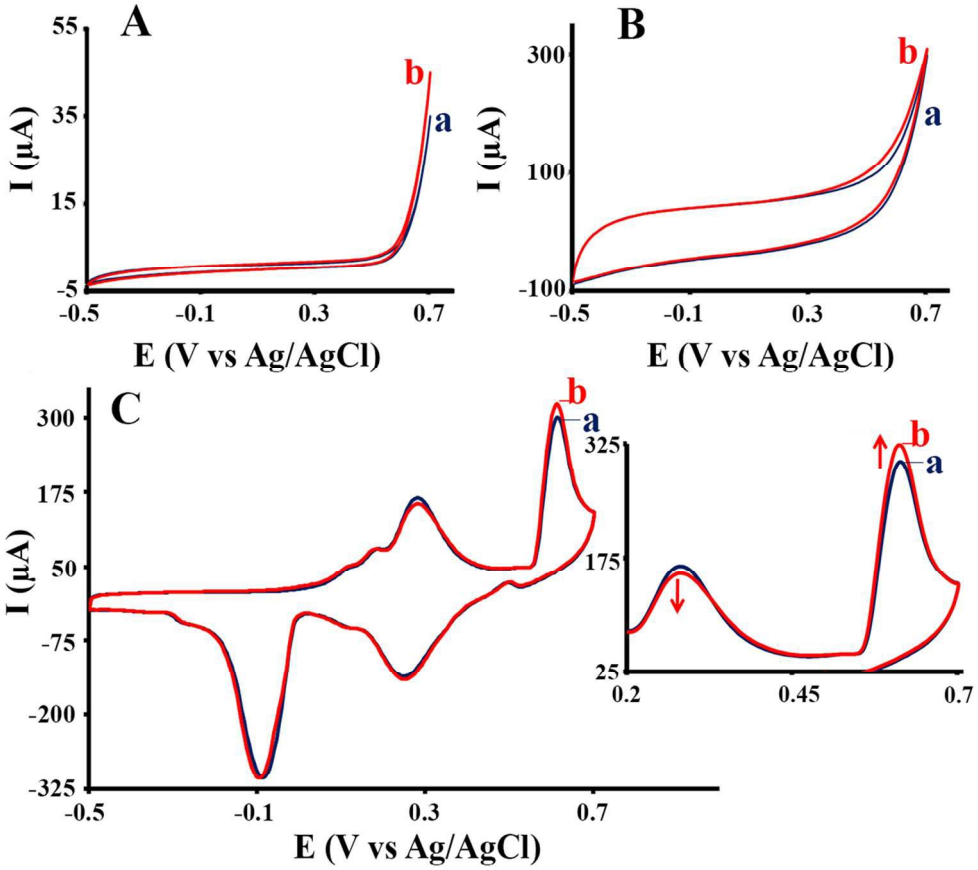

Fig. 4. Cyclic voltammograms of GCE (A), F–MWCNTs–GCE (B), and AgNPs/F–MWCNTs–GCE (C) in 0.1 M NaOH solution in the absence of glucose (a) and in the presence of 2.5 mM glucose solution at a scan rate of 50 mV s–1 (b).
136x123mm (300 x 300 DPI)

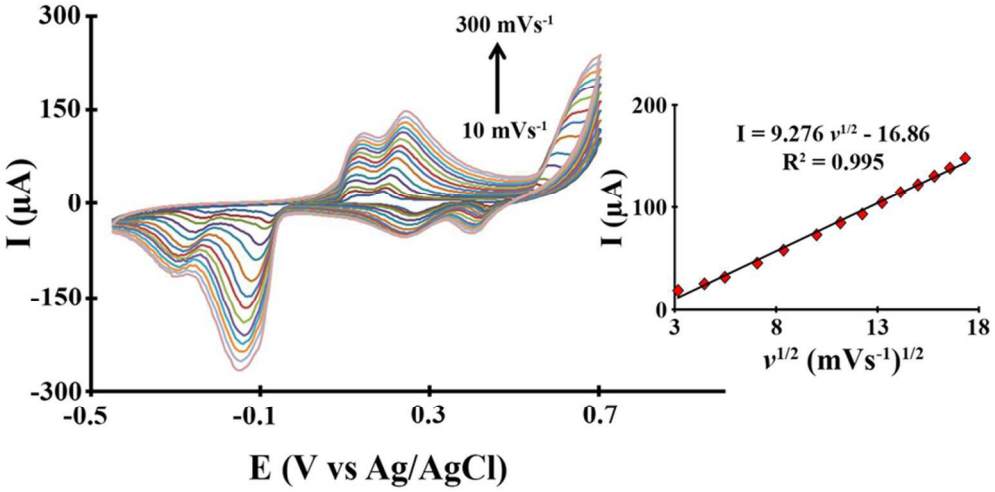

Fig. 5. The study of AgNPs/F–MWCNTs–GCE in 0.1 M NaOH solution and the presence of 5.0 mM glucose at the potential scan rate of 10–300 mV s–1. Inset: plot of the oxidation peaks vs. the square root of scan rates.
80x42mm (300 x 300 DPI)

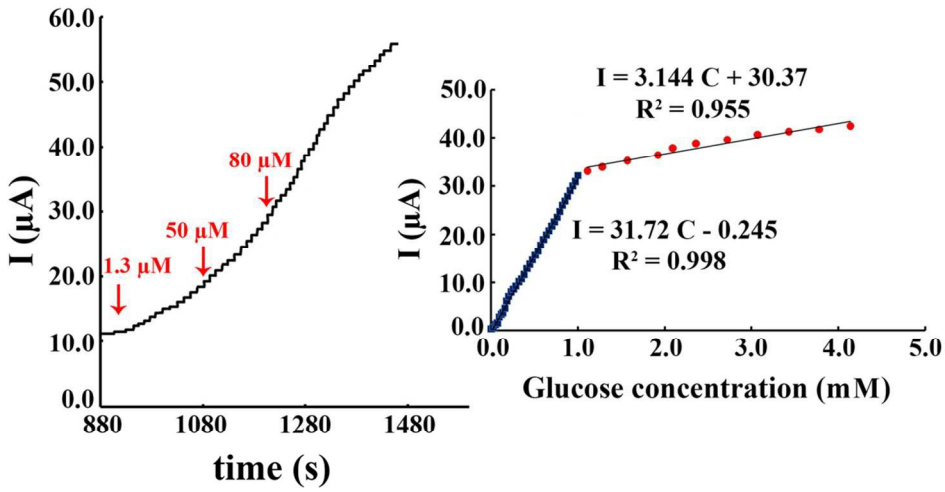

Fig. 6. Current–time study of AgNPs/F–MWCNTs–GCE vs. glucose addition in 0.1 M NaOH solution using hydrodynamic electrode at an applied potential of 0.58 V vs. Ag/AgCl and 1200 rpm with the corresponding two linear ranges of the calibration curve, showing in the inset.
109x60mm (300 x 300 DPI)

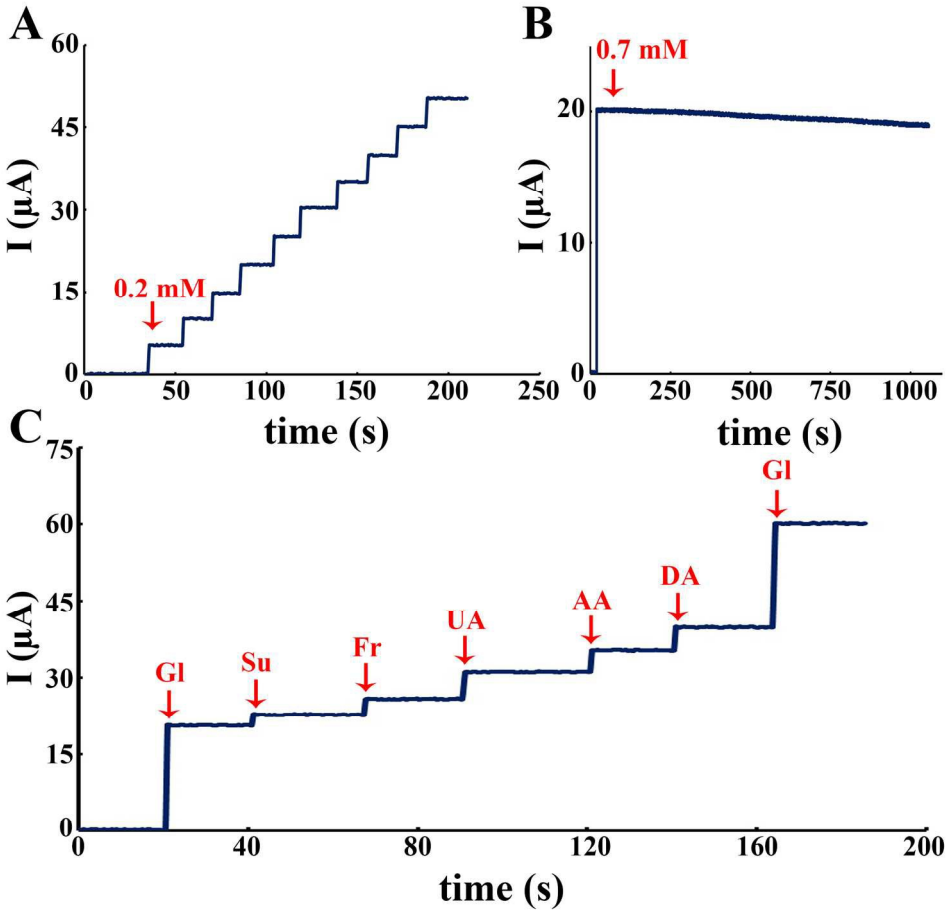

Fig. 7. Chronoamperometric study of the glucose oxidation current at AgNPs/F–MWCNTs–GCE in 0.1 M NaOH solution based on 10 successive additions of glucose solution (0.20 mM) (A); stability of the signal sensor until 1000 s by addition of glucose solution (0.70 mM) (B); and selectivity of the glucose sensor towards glucose solution (0.70 mM) in the presence of interfering species including sucrose (Su) (0.70 mM), fructose (Fr) (0.70 mM), Uric acid (UA) (0.07 mM), ascorbic acid (AA) (0.07 mM), and dopamine (DA) (0.07 mM) (C).
188x177mm (300 x 300 DPI)

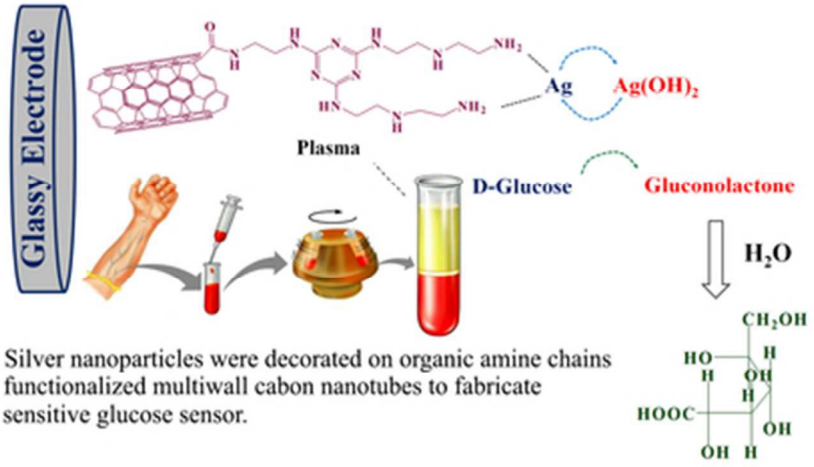

39x19mm (300 x 300 DPI)